People's Democratic Republic of Algeria
Ministry of Higher Education and Scientific research
M'hamed Bougara University, Boumerdes
Institute of Electrical and Electronic Engineering,
Laboratory of Signals and Systems (LSS)

ALGERIAN JOURNAL OF SIGNALS AND SYSTEMS

ISSN : 2543-3792

Title: **Emulation of metamatrial waveguides**

Authors: **Khedidja BOURAS, Abdelhadi LABIAD,Chaker SALEH, Mouloud BOUZOUAD**

Affiliation:
Electronic. Amar Telidji of Laghouat University (UATL), Laghouat, Algeria

Page range: **117-124**

Volume : 3 Issue : 3 (September 2018)

Laboratory of Signals and Systems
Address : IGEE (Ex-INELEC), Boumerdes University, Avenue de l'indépendance, 35000, Boumerdes, Algeria
Phone/Fax : 024 79 57 66
Email : lss@univ-boumerdes.dz ; ajsyssig@gmail.com

Emulation of metamatrial waveguides

Khedidja BOURAS(1)*, Abdelhadi LABIAD(2),Chaker SALEH(3), Mouloud BOUZOUAD(4)
Electronic. Amar Telidji of Laghouat University (UATL), Laghouat, Algeria
*kh.bouras@lagh-univ.dz

Abstract: In this work, we are interested by emulating metamaterial microwave waveguides which behave like conventional metallic ones. We use metamaterial layers based on two types of unit cells. The first one is a connected cross type unit cell which leads to a metamaterial with a near zero refraction index ($n_1 \approx 0$). The second one is a disconnected cross type unit cell which leads to a metamaterial with a refraction index greater than unity ($n_2 > 1$). With these two type of metamaterials we can define, in the metamaterial layer, different sections each one can have a refraction index equal to n_1 or n_2. Using these metamaterial layers we can build a metamaterial waveguide. This latter is obtained by stacking a number of layers. The waveguide is obtained by selecting an inner section with a refraction index n_2 and an outer section with a refraction index n_1 close to zero which plays a similar role as a metallic reflector to form the waveguide.

Keywords: Metamaterial, Waveguides, Refractive index, Dispersion diagram, Metamaterial waveguides.

1. INTRODUCTION

In recent years, metamaterials are widely used in telecommunication field. These artificial materials can improve the performance of microwave components such as antennas, transmission line, filters[1]-[5][16]. The theory study of the metamaterial of refractive index allows us to use it in several applications such as the cloaking [19], refractive index and light sensing [20][21], so the metamaterial devices involved special properties of magnetic permeability and dielectric permittivity to treat the phenomenon studied. The emulated waveguides based on metamaterial used in this work consisting two different refractive index extracted from a metamaterial unit cell which respected the sub-wavelength conditions [17][18] ,where its period is much smaller than the work wavelength. In this work we use a metamaterial based on a cross type unit cell. These unit cells are arranged in manner that all the crosses are connected (connected cross type metamaterial) or disconnected (disconnected cross type metamaterial). According to that the metamaterial can exhibit two different behaviors. The first one corresponds to the connected cross type unit cell, in which case the metamaterial behaves as a uniform medium with a refraction index close to zero ($n_1 \approx 0$). The second one corresponds to the disconnected cross type unit cell, in which case the metamaterial behaves as a uniform medium with a refraction index slightly greater than unity ($n_2 > 1$).Consequently, by stacking metamaterials layers, we can form a 3D bulk, formed by a hosting metamaterial with refraction index n_1 close the zero in which we can form a 3D shape which is filled with a metamaterial having a refractive index equal to n_2. This 3D shape can have the adequate geometrical design to emulate for example a circular or rectangular waveguide.

2. DESCRIPTION OF METAMATERIAL UNIT CELL

The cross unit cell is formed by two printed dipoles at 90° to each other, as shown in Fig. . This structure is arranged in a periodic fashion to constitute the metamaterial layer. In the case where the printed dipoles, forming the unit cross, have a length L, equal to the metamaterial period, all adjacent crosses forming the periodic structure are connected and hence, we obtain a connected cross type metamaterial. Otherwise, the printed dipoles have a length equal to L-g, where g is the gap between two adjacent crosses, in this latter case all the crosses forming the periodic structure are disconnected, and we obtain a disconnected cross type metamaterial. These two types of metamaterials (connected and disconnected cross type metamaterial) are used to design the metamaterial waveguide.
The metamaterial complex constitutive parameters are obtained by Fresnel inversion extraction method using the transmission and reflection coefficients derived by using home-mad or commercially available simulation code[10]. The dimensions of the elementary unit cell are represented in Fig. 1.

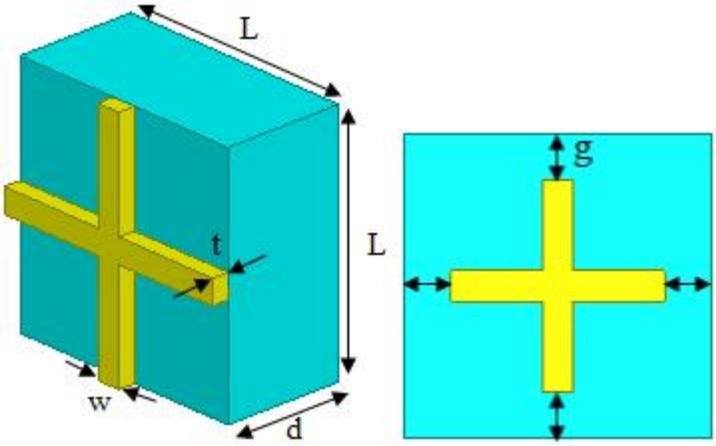

(a) (b)

Fig. 1 Elementary metamaterial unit cell (a) the connected cross (b) the disconnected cross: L = 0.711mm, w = 0.35 mm, t = 0.035 mm, d = 1.27 mm, g = 0.02 mm

The connected cross type metamaterial exhibits plasmatic-type permittivity frequency variation and follows Drude-type (non-resonant) frequency dependence [11]. For frequencies larger than the plasma frequency (f_p) the relative permittivity stays between 0 and 1. And negative for frequencies lower than the f_p. The connected cross metamaterial is positive and close to zero ($n_1 \approx 0$), as shown in Fig -c. The disconnected cross type metamaterial exhibits a Lorentz type (resonant) frequency variation [14]-[15]. The refractive index is slightly greater than unity (n_2 = 1.95).

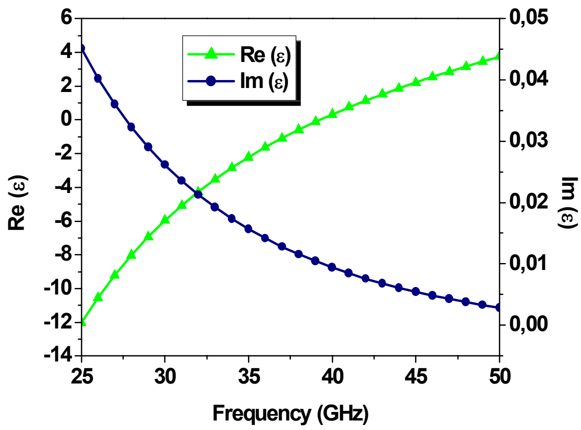

(a)

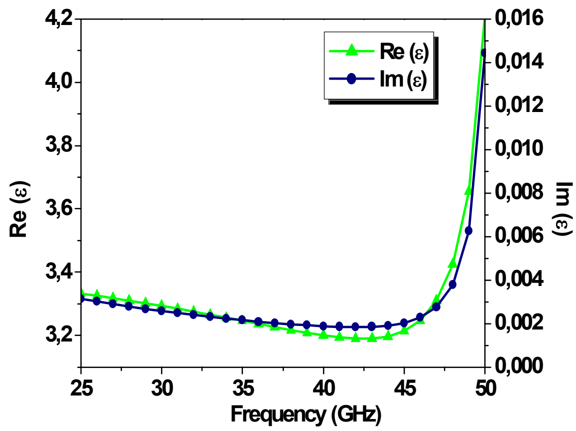

(d)

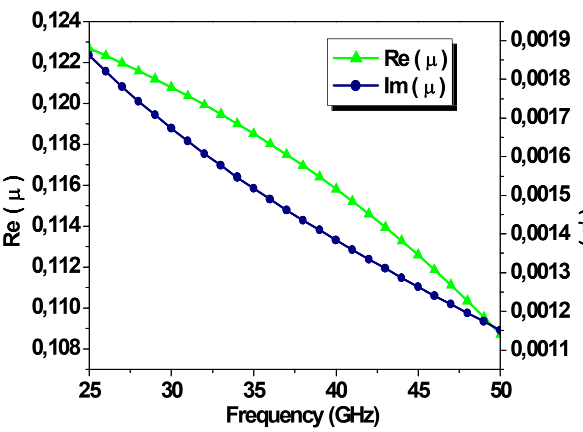

(b)

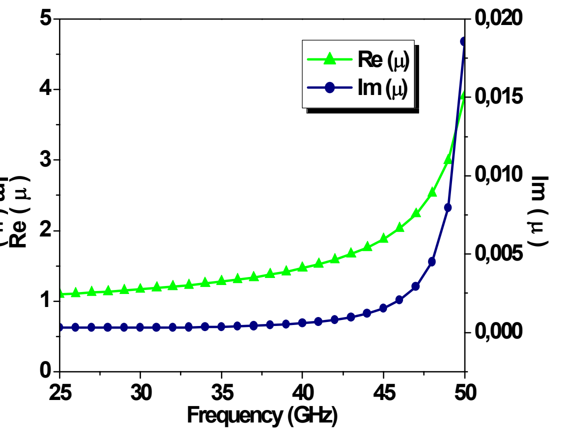

(e)

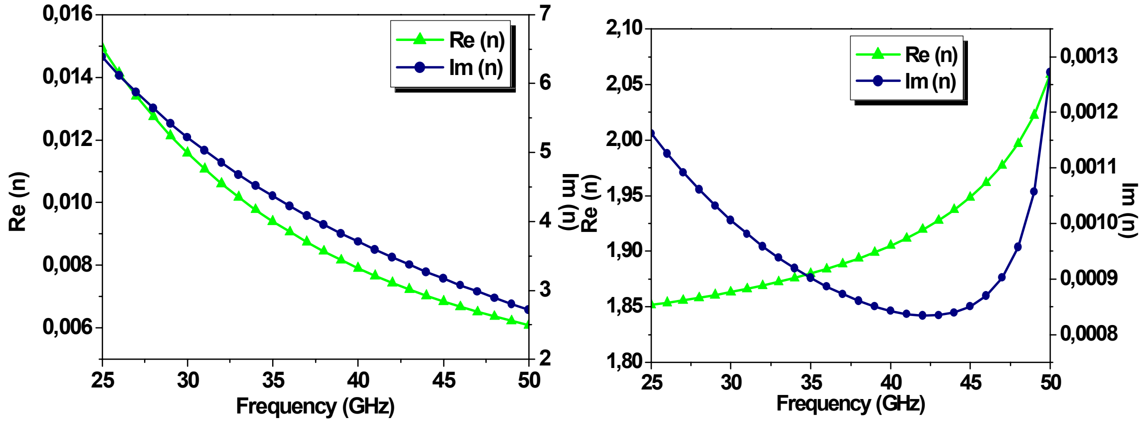

(c) (f)

Fig 2 The constitutive parameters on the order are (a), (b), (c) for the connected cross and (d), (e), (f) for the disconnected cross.

3. EMULATION OF METAMATERIAL WAVEGUIDE

The emulated waveguide is a block composed by a stack of metamaterial layers. Each layer is composed by a periodic arrangement of metal cross pattern printed on a dielectric substrate. In each layer we can differentiate two areas, the first one form the inner section of the metamaterial waveguide and the second area forms the outer section of the metamaterial waveguide.

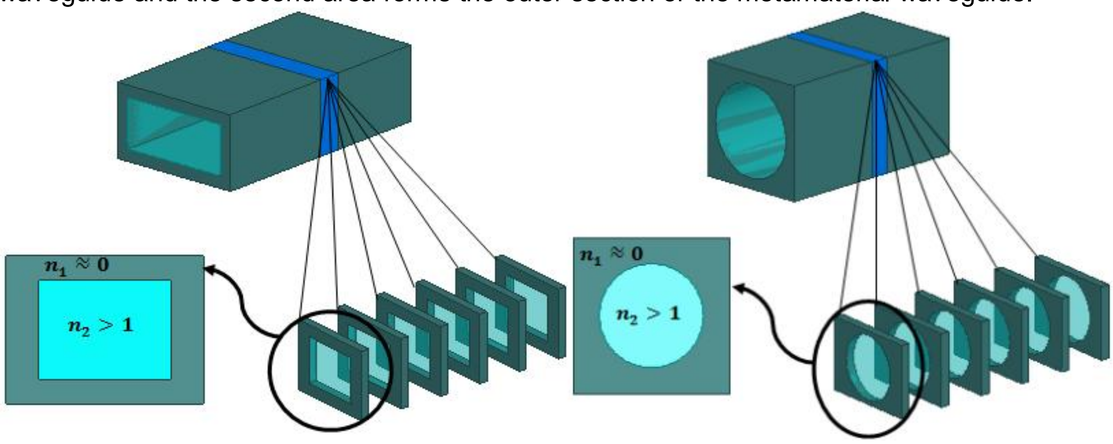

(a) (b)

Fig.3The 3D bulk metamaterial waveguide (a) rectangular (b) circular waveguide

The waveguide inner section, based on disconnected cross type metamaterial (n_2 = 1.95), can have any arbitrary shape (Rectangular, circular, elliptic…) and form the medium filling the waveguide. The remaining area, in the metamaterial layer, forms the outer section based on connected cross type metamaterial ($n_1 \approx 0$), as shown inFig..

4. RESULTS AND DISCUSSIONS

4.1. Rectangular waveguide emulation

In this work we simulate the standard rectangular waveguide WR-22, its inner dimensions are a = 5.69 mm, b = 2.845 mm. The cutoff frequency calculated using equation$f_{c_{mn}} = \frac{c}{2}\sqrt{(\frac{m}{a})^2 + (\frac{n}{b})^2}$. () is fc_{10} = 26.36 GHz for TE_{10} dispersion mode [8][12][13]:

$$f_{c_{mn}} = \frac{c}{2}\sqrt{(\frac{m}{a})^2 + (\frac{n}{b})^2}. \quad (1)$$

The metamaterial waveguide inner section has the same dimensions (a x b) as the conventional metallic one. To form this rectangular section we need a matrix of 8 x 4 unit cells as shown in Fig. 4.

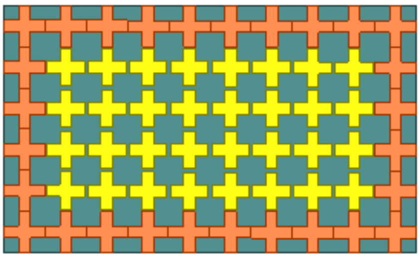

Fig.4 One grid matrix of 8 x 4 cross section

Each unit cell is a square area of L x L mm^2 (L = 0.711 mm = 1 unit cell). The Dispersion diagrams of the conventional WR-22 metallic and the 8 x 4 unit cells metamaterial rectangular waveguide as shown in
Fig..
The metamaterial rectangular waveguide cutoff frequencies are given by [6][9]

$$f_{c_{mn\,MTM}} = \frac{f_{c_{mn}}}{\sqrt{n_2{}^2 - n_1{}^2}} \tag{2}$$

From equations (1) and (2), the following can be obtained:

$$f_{c_{mn\,MTM}} = \frac{c}{2}\sqrt{\left(\frac{m}{a\sqrt{n_2{}^2-n_1{}^2}}\right)^2 + \left(\frac{n}{b\sqrt{n_2{}^2-n_1{}^2}}\right)^2} \tag{3}$$

Which it can be written as:

$$f_{c_{mn\,MTM}} = \frac{c}{2}\sqrt{\left(\frac{m}{A}\right)^2 + \left(\frac{n}{B}\right)^2} \tag{4}$$

Where:

$$A = a\sqrt{n_2{}^2 - n_1{}^2} \tag{5}$$

And

$$B = b\sqrt{n_2{}^2 - n_1{}^2} \tag{6}$$

The metamaterial waveguide dimensions are reduced by a factor equal to $\sqrt{\mathbf{n}_2{}^2 - \mathbf{n}_1{}^2}$ as show the equations (5) and (6), where n_1 is close to zero and n_2 is equal to 1.95. In the case of our study the used metamaterial has a refraction index of n_2, the metamaterial waveguide inner section is reduced by a factor of 1.95 and is obtained by a matrix of 4 x 2 unit cells only.

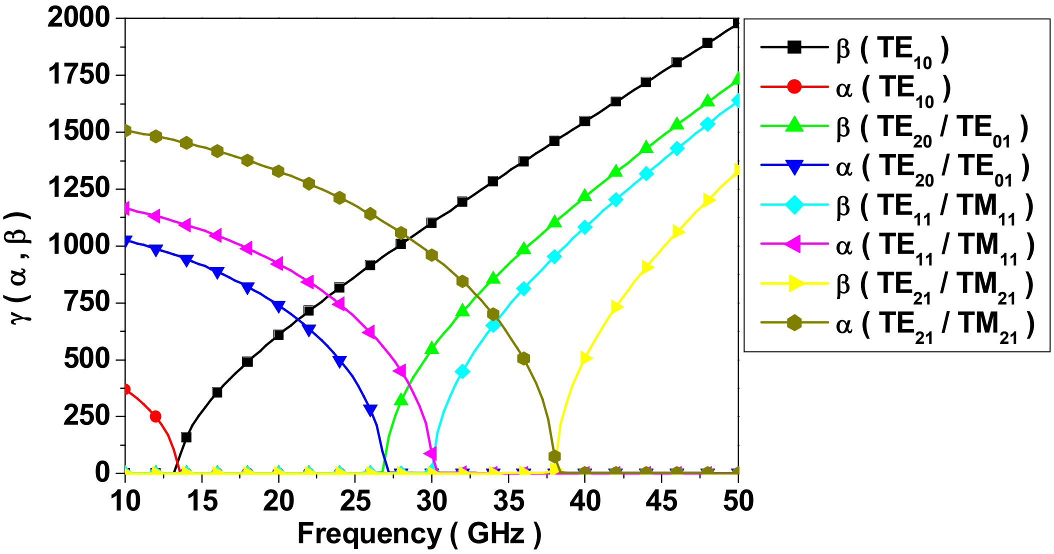

Fig. 5 The first seven modes of the metamaterial WR-22 rectangular waveguide for an inner section of 4 x 2 unit cells.

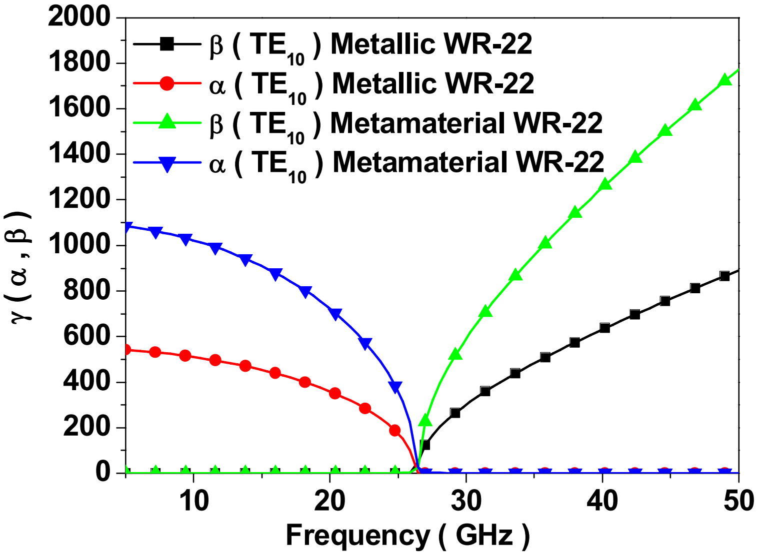

Fig.6 Dispersion diagrams comparison between the conventional and Metamaterial WR-22

Table 1 summarizes the cutoff frequencies of the first seven modes for the metallic, theoretical calculation and the emulated WR-22 waveguide, which was represented in Fig. 5.

Table 1 TE and TM dispersion modes cutoff frequencies of the conventional WR-22*Circular waveguide emulation*

Modes	$f_{c0_{nm}}(GHz)$ Metallic WR-22	$f_{c_{nm_{MTM}}}(GHz)$ MTM WR-22 (4 x 2) units cell	$f_{c_{nm_{MTM}}}(GHz)$ MTM WR-22 (8 x 4) units cell	$f_{c_{nm_{MTM}}}(GHz)$
TE_{10}	26.37	26.45	13.25	13.52
TE_{01}	52.8	53.4	26.45	27.07
TE_{20}	52.8	53.4	26.45	27.07
TE_{11}	59.03	59.45	29.75	30.27
TM_{11}	59.03	59.45	29.75	30.27
TE_{21}	74.63	76.2	38.1	38.27
TM_{21}	74.63	76.2	38.1	38.27

We use the same procedure to simulate the C255 (R = 4.165mm) standard metallic circular waveguide [7]. The inner section of the metamaterial waveguide is obtained by a circular shape of diameter R equal to 12 times the unit cell, inscribed in a grid matrix of 12 x12 disconnected cross unit cells, as shown in Fig. 7.

Dispersion diagrams of the dominant TE_{11} mode of both conventional C255 metallic waveguide and the 6 cells radius circular metamaterial waveguide inner section are shown in Fig. 8.

$$f_{c_{mn}} = \frac{C}{2\pi}\frac{X_{mn}}{R\sqrt{\varepsilon_r\mu_r}} \tag{7}$$

Where, $\mathbf{X_{mn}}$ are the zeroes of the derivatives $\mathbf{J'(X_{mn}) = 0}$ of Bessel function, R is the circle radius.

The metamaterial circular waveguide cutoff frequencies can be written as [6]:

$$f_{c_{mn}} = \frac{C}{2\pi}\frac{X_{mn}}{R\sqrt{{n_2}^2-{n_1}^2}} \tag{8}$$

$$f_{c_{mn}} = \frac{C}{2\pi}\frac{X_{mn}}{R'} \tag{9}$$

According to equation the circular metamaterial waveguide inner section diameter is smaller compared to that of the conventional metallic one. To obtain the same cutoff frequency as the C255 metallic waveguide of radius R, the metamaterial one should have a radius R' equal to R divided by a factor equal to $\sqrt{{n_2}^2 - {n_1}^2}$[9]. In the case where n_2 = 1.95 and, n_1≈ 0, R' is equal to 2.136 mm inner which is 3 time the unit cell. A comparison of dispersion diagrams of the metamaterial circular waveguide of radius R' compared to that of the conventional metallic is represented in Fig. 9.

We note a good agreement for the cutoff frequencies. The metamaterial dominant mode cutoff frequency obtained by simulation and by equation (2) agrees well [12][13], as it can be seen in table 2. The metallic circular waveguide TE mode cutoff frequencies given by [8]:

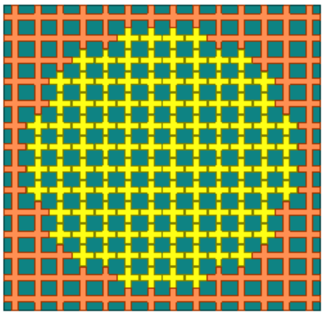

Fig.7 One grid matrix of 12 x12 disconnected cross unit cells in the inner section diameter

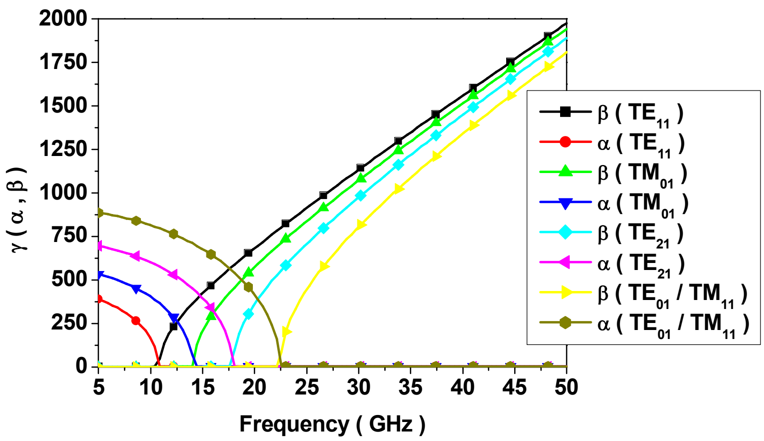

Fig.8 The first five dispersion diagrams of the metallic and metamaterial C255 waveguide with an inner section of 12 disconnected cross unit cell diameter

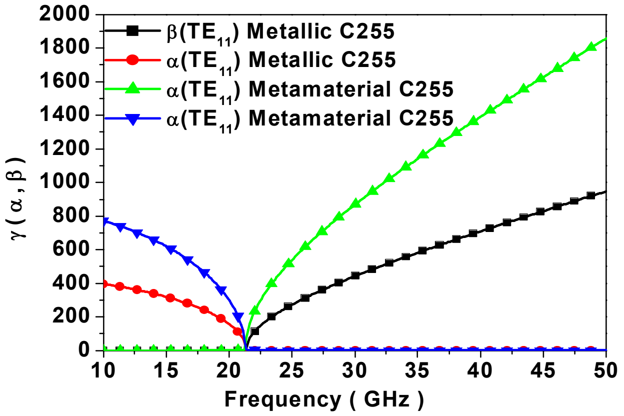

Fig. 9 Dispersion diagrams of the metallic C255 and metamaterial circular waveguide of an inner section diameter of 6 disconnected cross unit cell

Table 2 The first five dispersion diagrams of the metallic and metamaterial C255 waveguide

Modes	$f_{c0_{mn}}$(GHz)	$f_{c_{mn_{MTM}}}$(GHz) 3 unit cells radius inner section	$f_{c_{mn_{MTM}}}$(GHz)	$f_{c_{mn_{MTM}}}$(GHz) 6 unit cells radius inner section
TE_{11}	21.2	21.5	10.87	10.68
TM_{01}	27.6	28.19	14.15	14.15
TE_{21}	35.2	35.8	18.05	17.75
TE_{01}	44.15	44.89	22.64	22.55
TM_{11}	44.15	44.89	22.64	22.55

5. CONCLUSIONS

In this work we have use two type of metamaterial unit cells. These unit cells have a very close geometrical design but exhibit two different electromagnetic behaviors. The first one is a connected cross type unit cell which leads to a metamaterial behaving as a uniform medium with a refraction index close to zero and follows a Drude-type (non-resonant) model. The second one is a disconnected cross type unit cell which leads to a metamaterial behaving as a dielectric with are fraction index greater than unity and follows a Lorentz-type (resonant) model. With these two types of metamaterials. We have designed a 3D metamaterial bulk which can emulate any shape of waveguides. We have design a circular and rectangular metamaterial waveguide to emulate the metallic WR-22 rectangular and C255 circular waveguides. The obtained results agree well especially for the TE dominant mode cutoff frequency.

References

[1] L. Solymar and E. Shamonina, “Waves in Metamaterials.” Oxford, NewYork: Oxford University Press, 2014.

[2] Y.Zou, L.Jiang, Sh.Wen ,Y.Qing, Zh.Tang, W.Shu, H.Luo, and D.Fan “Enhancingmicrowave absorption properties of materials using metamaterials”IEEE Xplore Document, 2008.

[3] Okeke, C, Emole, E.C, Anorue, E. N,“Miniaturization of MicrowaveDevices: It’s Effect in Improving Electronic Circuits” Vol. 4 Issue 2 July2014.

[4] Jeffrey R. Clark,“Double Negative Metamaterials in DielectricWaveguide Configurations”, Virginia Polytechnic Institute and StateUniversity in partial fulfillment of the requirements for the degree ofDoctor of Philosophy ,2006.

[5] H. J. El-Khozondar , R. J. El-Khozondar, M. M. Shabat “Doublenegativemetamaterial optical waveguide behavior subjected to stress”,Proc. SPIE 6987, Metamaterials III, 69871W 2008.

[6] Z.S.A. Mebark, “Support de transmission et composant micro-ondes, ”OPU,1995.

[7] F. Gardiol, “Traité de l’Electricité, ” volume III, Georgi, 1981.

[8] Devendre, k.Misra “Practical electromagnetics from biomedical sciencesto wireless communication”, Published by John Wiley & Sons, Inc.,Hoboken, New Jersey. University of Wisconsin, 2007.

[9] M.Skorobogatiy, “Nanostructured and Subwavelength Waveguides: Fundamentals and Applications”, John Wiley & Sons, 2012.

[10] Smith, D.R. and Schultz, S., Markos, P., Soukoulis, C.M, “Determination of effective permittivity and permeabilityof metamaterials from reflexion and transmission coefficients” Phys. Rev. B, 65, 2002.

[11] Tie Jun, S.David, L.Ruopeng, “Metamaterials: Theory, Design, and Applications”, Springer Science & Business Media, 2009.

[12] Pozar, David M, “Microwave Engineering”, 2nd edition, John Wiley & Sons, 1997.

[13] R.E. Collin, “founfations of microwave engineering, 2nd edition, IEEE Press Series-John Wiley & Son, 2001.

[14] JG. Rivas, J.A . Snchez-Gil, M. Kuttge,Ph. Bolivar, H. Kurz, “Optically switchable mirrors for surface plasmon polaritons propagating on semiconductor surfaces”, Phys Rev B74:245–324, 2006.

[15] I. Ahmed, E. KHoo, O. kurniawan, E. Li, “Modeling and simulation of active plasmonics with the FDTD method by using solid state and Lorentz–Drude dispersive model”, Optical Society of America, 2011.

[16] M.Bouzouad, C.Saleh, D. Bensafielddine,and M. Laamari, “Gain enhancement with near-zero-index metamaterial superstrate”, Applied Physics A.121, 2015.

[17] Hou, L.L, Chin, J.Y, Yang, X.M, Lin, X.Q, Liu, R, Xu, F.Y, Cui, T.J: Advanced parameter retrievals for metamaterial slabs using an inhomogeneous model. J. Appl. Phys. 103, 064904, 2008

[18] Schurig, D., Mock, J.J., Justice, B.J., Cummer, S.A., Pendry, J.B., Starr, A.F., Smith, D.R.: “Metamaterial electromagnetic cloak at microwave frequencies”. Science 314, 977–980, 2006

[19] I.Smolyaninov, V.N Smolyaninova, A.Kildishev, and V.M Shalaev, “A Near Zero Refractive Index Metamaterial for Electromagnetic Invisibility Cloaking Operation”, Materials, 8,2015.

[20] Y.Lee, S.J.Kim, H.Park and B.Lee, “Metamaterials and Metasurfaces for Sensor Applications”, Sensors,2017.

[21] N.Vasilantonakis, M.E. Nasir, W.Dickson, G.A. Wurtz, and A.V. Zayats, “bulk plasmon-polaritons in hyperbolic nanorod metamaterial waveguides”, Laser Photonics Rev. 9, No. 3, 345–353, 2015.